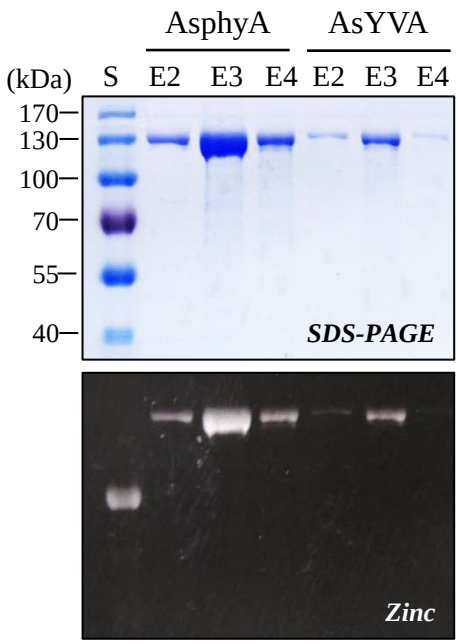

Supplemental Figure S1. Purified recombinant wild-type (AsphyA) and Y268V-AsphyA (AsYVA) proteins used in the photochemical analysis. Recombinant phytochrome proteins with a ten-amino acid streptavidin affinity tag (~127 kDa) were expressed in *Pichia pastoris* cells (1 liter culture) and purified after addition of phycocyanobilin (PCB) as the chromophore using streptavidin affinity chromatography. Lane S, PageRuler prestained protein ladder (Fermentas); lanes E2-E4, elution fractions (0.5 mL each) of purified AsphyA and AsYVA proteins. Ten microliters of each elution fraction were used for SDS-PAGE, and zinc fluorescence (Zinc) was shown to confirm the ligation of the chromophore to the phytochrome protein. It is notable that the expression level of AsYVA was much lower than that of wild-type AsphyA, but the chromophore ligation appeared to be normal when comparing the intensities of zinc fluorescence with the protein bands in SDS-PAGE.

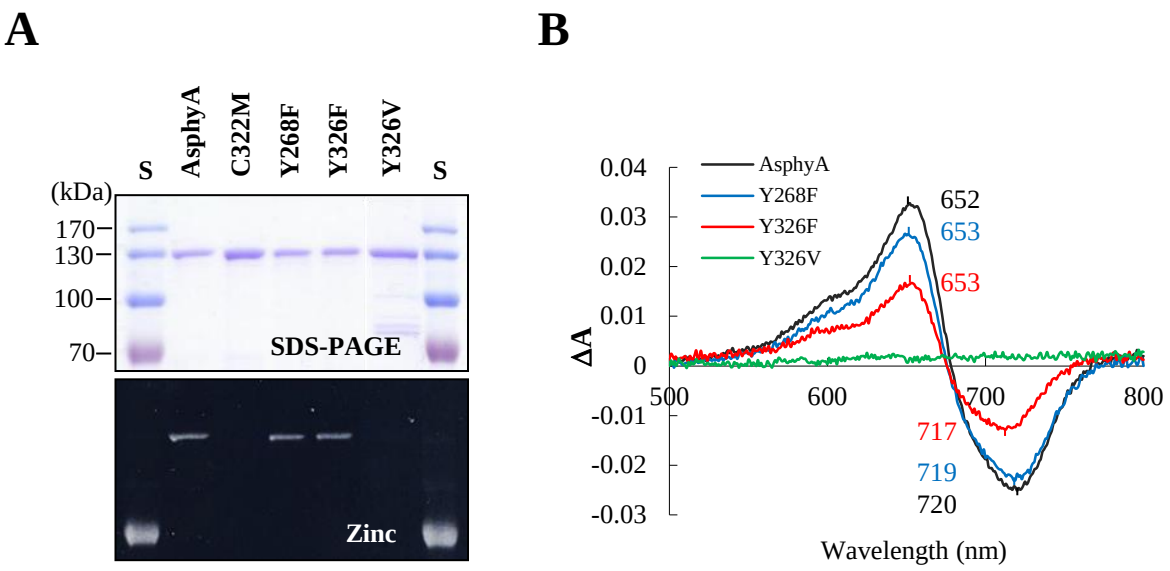

Supplemental Figure S2. Photochemical analyses of purified recombinant AsphyA mutant proteins. **A**, Zinc fluorescence assays to show chromophore ligation in the AsphyA proteins. All the proteins were expressed in *P. pastoris* cells and purified after addition of PCB as the chromophore using the streptavidin affinity chromatography. Lane S, PageRuler prestained protein ladder (Fermentas); AsphyA, wild-type *A. sativa* phyA; C322M, Cys322-to-Met mutant of AsphyA; Y268F, Tyr268-to-Phe mutant; Y326F, Tyr326-to-Phe mutant; Y326V, Tyr268-to-Val mutant. C322M is the chromophore-binding site mutant and included as a negative control for chromophore ligation. It is notable that the chromophore-ligated phytochromes displayed pink bands under UV light, whereas one white band (70 kDa) was observed from the protein standards. **B**, Difference spectra of the AsphyA mutants. No difference spectrum was observed in the Y326V mutant (green), while the Y268F (blue) and Y326F (red) mutants displayed similar difference spectra to wild-type AsphyA (black). The absorption maxima are also indicated.

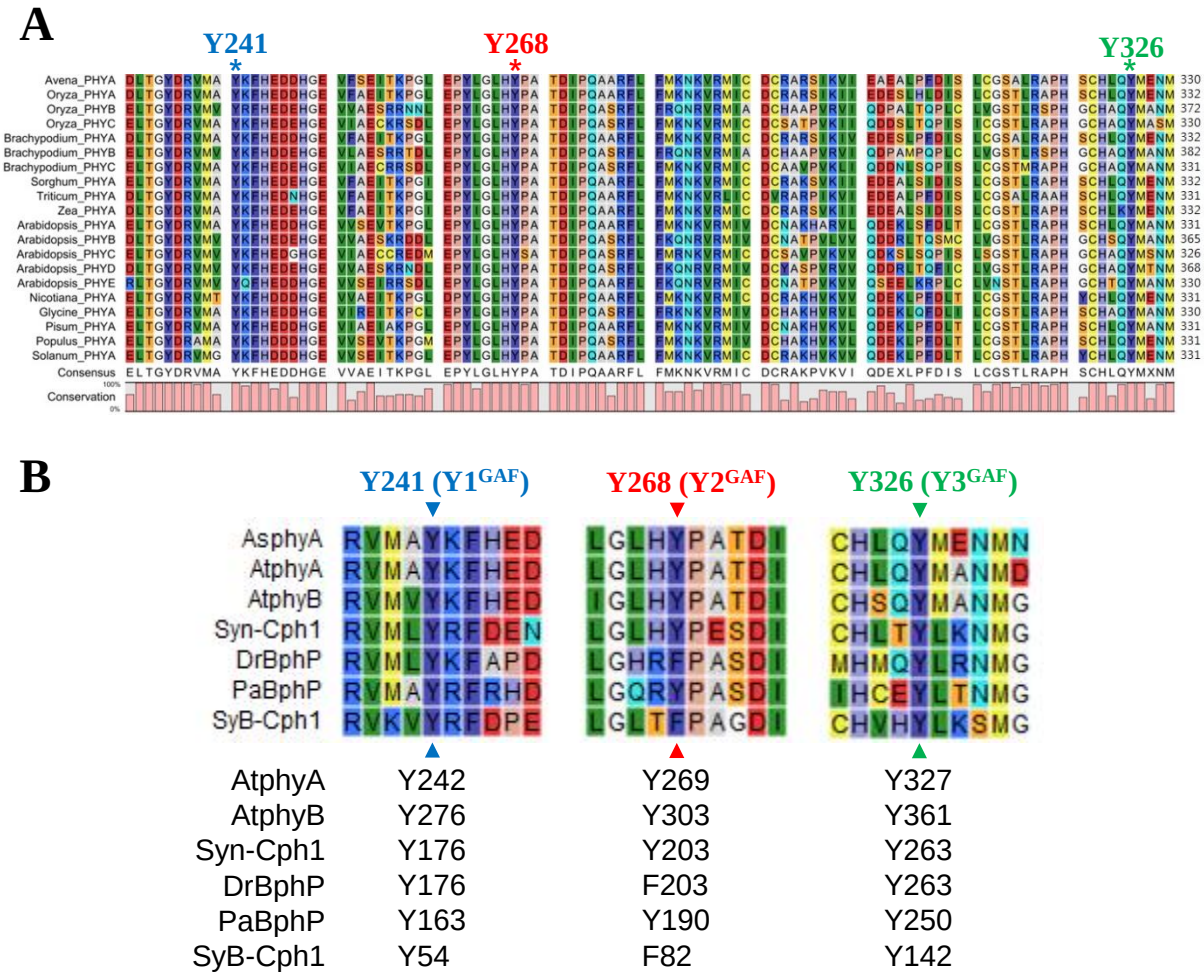

Supplemental Figure S3. Amino acid sequence alignments of phytochromes. **A**, The sequence alignment using plant phytochromes. The sequences that belong to the GAF domain (217-401aa in the case of AsphyA) are obtained from diverse taxa (10 monocotyledonous and 10 dicotyledonous plant species) and used for the alignment using CLC Main Workbench. The Y241, Y268, and Y326 residues of AsphyA are indicated with blue, red, and green asterisks, respectively. It is notable that the Y241 residue of AsphyA corresponds to Y242-AtphyA and Y276-AtphyB, the alleles previously used to generate constitutively active phytochromes. **B**, Alignments of the sequences containing Y241, Y268, and Y326 residues of AsphyA. Corresponding Tyr residues of AtphyA and AtphyB to AsphyA are presented below the alignments. In addition, the Tyr residues in the bacterial phytochromes with available structures are also presented. Syn-Cph1, the cyanobacterial phytochrome from *Synechocystis* PCC 6803 (GenBank No. BAA10307.1); DrBphP, *Deinococcus radiodurans* bacteriophytochrome (GenBank No. AAF12261.1); PaBphP, *Pseudomonas aeruginosa* bacteriophytochrome (GenBank No. EAZ54446.1); SyB-Cph1, the cyanobacterial phytochrome from *Synechococcus* OSB′ (GenBank No. ABD03399.1).

A

AsphyA or AsYVA

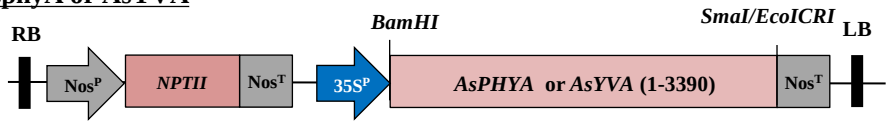

AsphyA:eGFP or AsYVA:eGFP

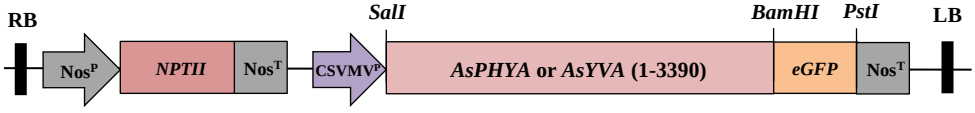

AsYVA:eGFP/NLS

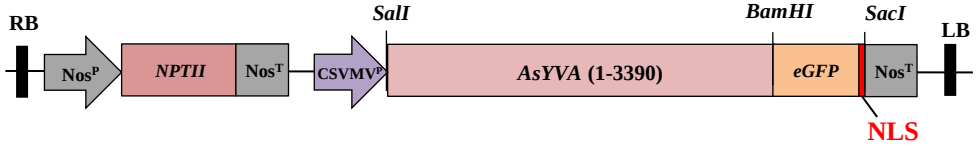

B

AtphyB, AtYVB, or YHB

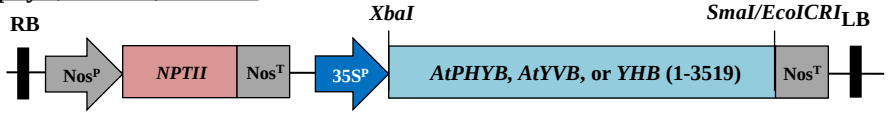

AtphyB:eGFP or AtYVB:eGFP

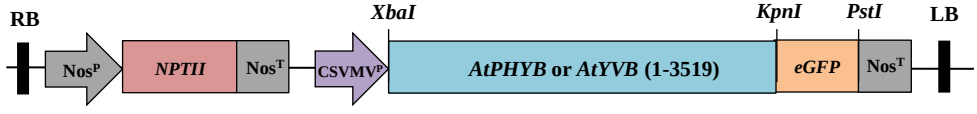

AtYVB:eGFP/NES

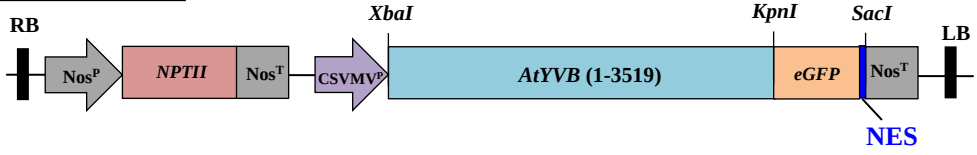

C

AtphyA:eGFP or AtYVA:eGFP

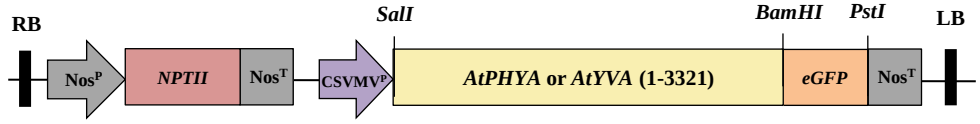

Supplemental Figure S4. T-DNA regions of the binary vector constructs used for plant transformation. **A**, T-DNA regions of the constructs for *Avena sativa* phyA. LB, left border sequence; RB, right border sequence; NOS^P, NOS (nopaline synthase) promoter; NOS^T, NOS transcriptional terminator; *NPTII*, neomycin phosphotransferase II gene; $35S^P$, cauliflower mosaic virus 35S promoter; $CsVMV^P$, cassava vein mosaic virus promoter; *eGFP*, enhanced GFP gene. AsphyA and AsYVA cDNAs were cloned into pBI121, pBI121-eGFP, and pBI121-eGFP/NLS vectors. NLS (nuclear localization signal) was fused to the C-terminal end of the eGFP-fused AsYVA to generate AsYVA:eGFP/NLS. **B**, T-DNA region of the constructs for *Arabidopsis thaliana* phyB. Wild-type AtphyB and AtYVB cDNAs were cloned into pBI121, pBI121-eGFP, and pBI121-eGFP/NES vectors. NES (nuclear export signal) was fused to the C-terminal end of the eGFP-fused AtYVB to generate AtY303V:eGFP/NES. **(C)** T-DNA region of the constructs for *A. thaliana* phyA. Wild-type AtphyA and AtYVA cDNAs were cloned into the pBI121-eGFP vector.

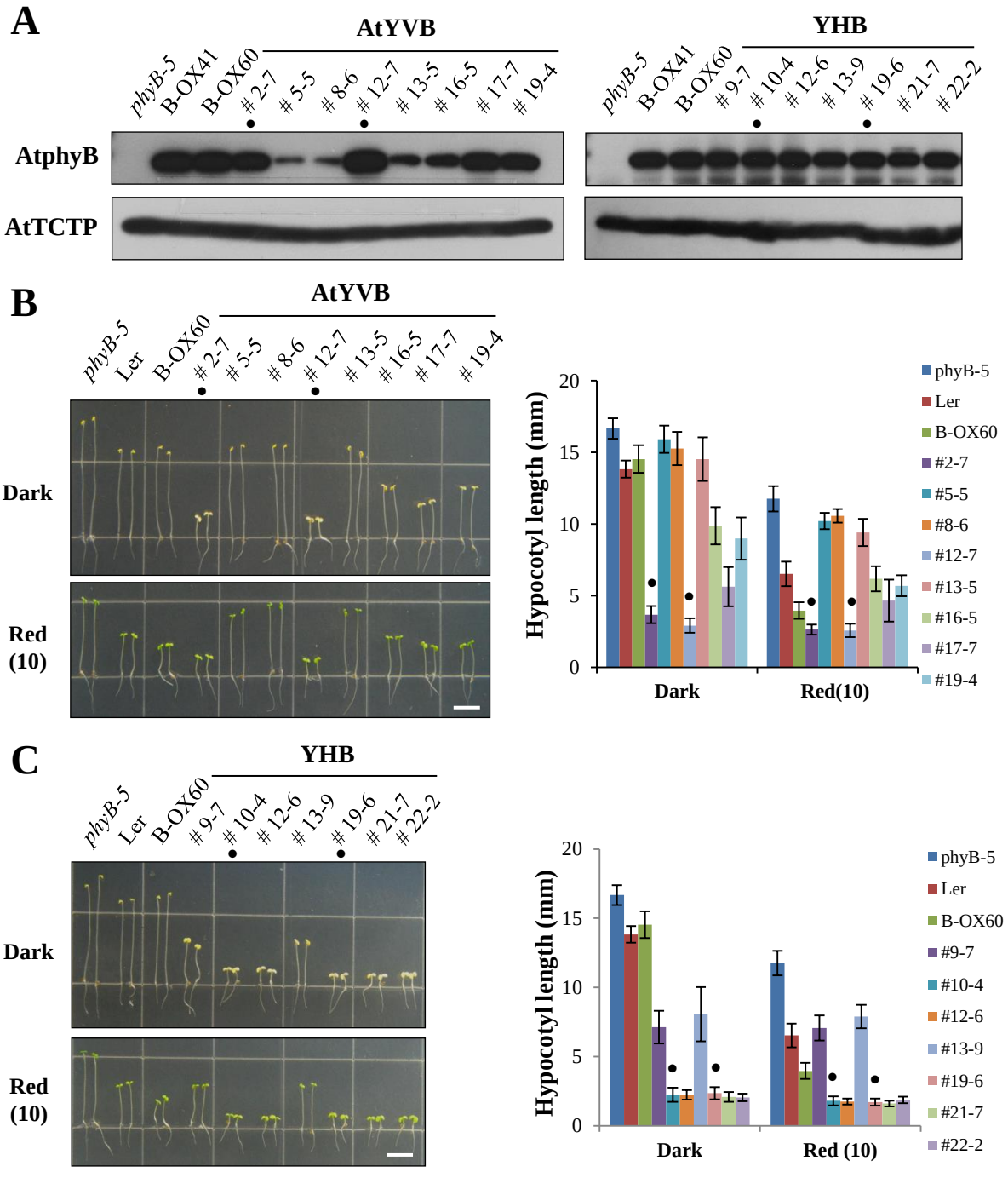
A
AtYVB
YHB
phyB-5
B-OX41
B-OX60
#2-7
#5-5
#8-6
#12-7
#13-5
#16-5
#17-7
#19-4
#9-7
#10-4
#12-6
#13-9
#19-6
#21-7
#22-2
AtphyB
AtTCTP
B
Ler
Dark
Red (10)
Hypocotyl length (mm)
Red(10)
C
Red (10)

Supplemental Figure S5. Transgenic *phyB-5* plants expressing AtYVB and YHB. **A**, Immunoblot analysis to show the protein levels of AtphyB in transgenic plants. *phyB-5*, phyB-deficient *A. thaliana* (L*er* ecotype); B-OX, transgenic *phyB-5* lines overexpressing wild-type AtphyB; AtYVB, transgenic *phyB-5* lines with Y303V-AtphyB; YHB, transgenic *phyB-5* lines with Y276H-AtphyB. Numbers represent independent homozygous lines. An AtphyB-specific (aN-20) antibody was used for the detection of AtYVB and YHB, as well as wild-type AtphyB. Loading controls (AtTCTP) are shown in lower panels. **B-C**, Hypocotyl de-etiolation of seedlings of the AtYVB (B) and YHB (C) plants under dark or continuous red light (10 µmol m^{-2} s^{-1}). Scale bar = 5.0 mm. Graphs show the average hypocotyl lengths of seedlings. Data are the means ± SD ($n \geq 30$). Filled circle indicate the representative lines used in further analyses.

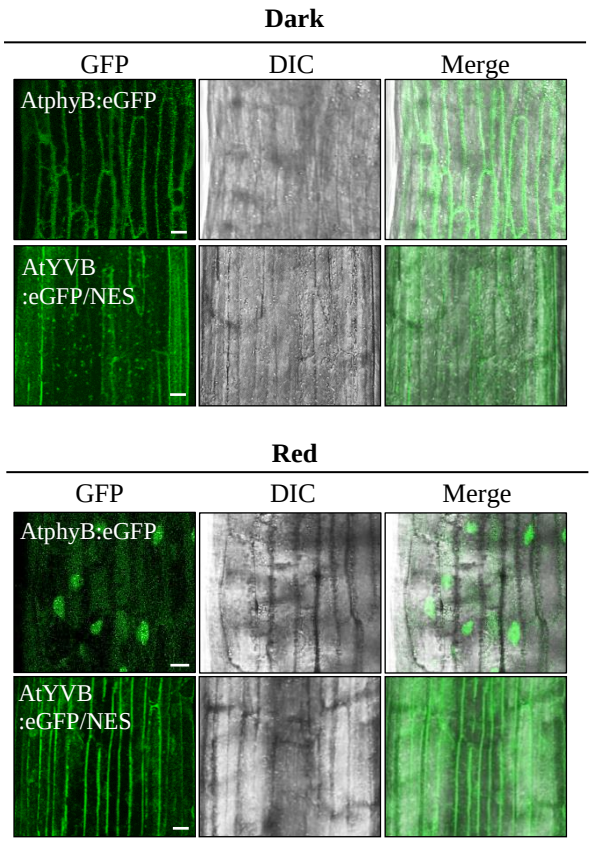

Supplemental Figure S6. Nuclear localization of NES-fused AtYVB. 3-d-old dark-grown transgenic seedlings of AtphyB:eGFP and AtYVB:eGFP/NES were kept in the dark or exposed to red light (5.0 μmol m^{-2} s^{-1}) for 1 h. DIC, different interference contrast. Scale bar = 10 μm.

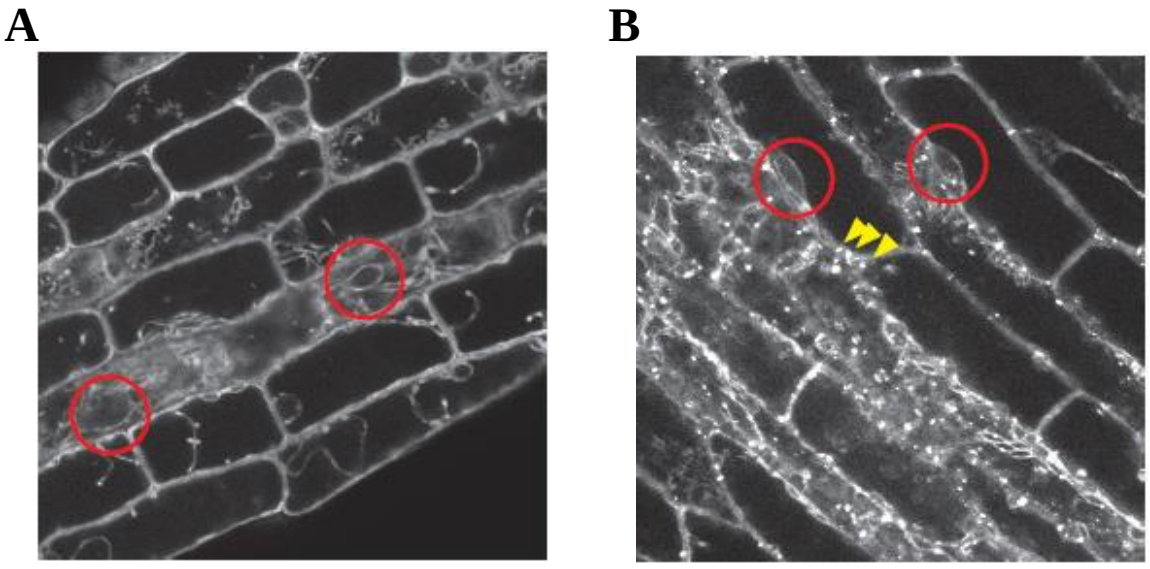

Supplemental Figure S7. Subcellular localization analyses of wild-type AsphyA (**A**) and AsYVA (**B**). For the confocal microscopic observations, 3-d-old dark grown seedlings were used. Red circles indicate empty nuclei, and yellow arrowheads indicate cytoplasmic speckles. In our experimental conditions, little nuclear localization of AsYVA was observed in the dark. Rather, we observed cytosolic speckles.

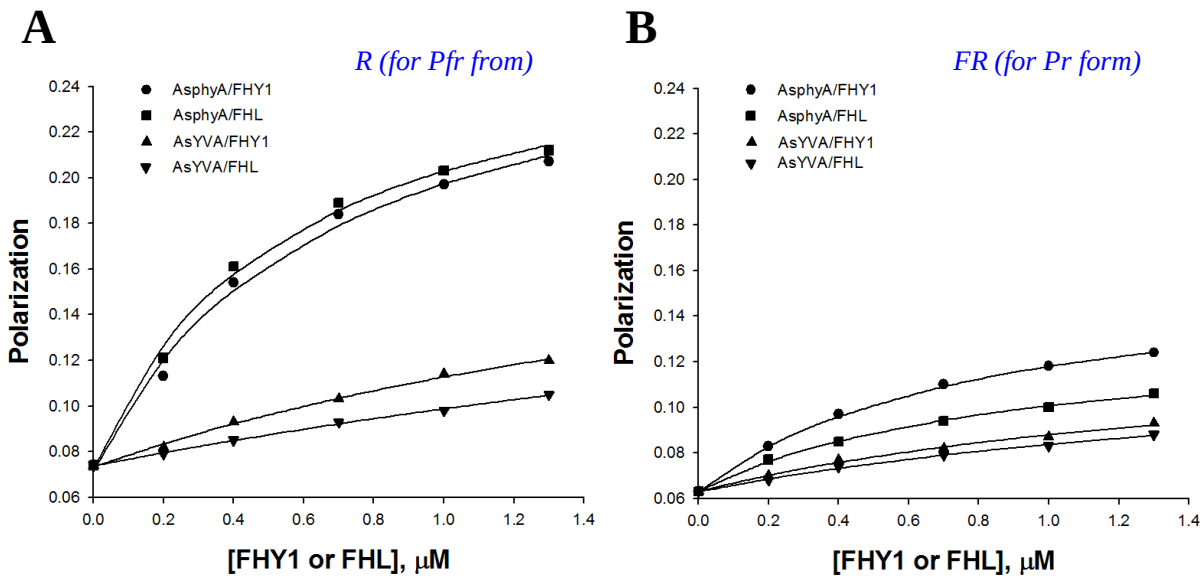

Supplemental Figure S8. Determination of dissociation constants for the protein-protein interaction between AsphyA/AsYVA and FHY1/FHL. After saturating irradiation by R (**A**) and FR (**B**), AsphyA and AsYVA proteins were labeled with IAEDANS (protein/probe = 0.4). Then, 0.5 μM of IAEDANS-labeled AsphyA/AsYVA was mixed with increasing concentrations of FHY1 or FHL. The dissociation constants (K_d values) were then calculated from the measurements of fluorescence polarization (P). The K_d values for the Pfr form of AsphyA were calculated to be 0.66×10^{-6} M for FHY1 and 0.54×10^{-6} M for FHL, and those for the Pr form were approximately 2.81×10^{-6} M and 2.90×10^{-6} M. The K_d values for the R-irradiated AsYVA were calculated to be approximately 6.68×10^{-6} M for FHY1 and 8.34×10^{-6} M for FHL. FR-irradiated AsYVA also showed similar K_d values (~7×10^{-6} M) to R-irradiated AsYVA. It should be noted that we could not obtain a saturable binding with AsYVA, as well as the Pr form of AsphyA, within the tested range of FHY1/FHL concentrations. Thus, the K_d values of AsYVA and the Pr form of AsphyA are estimates using the equation in the Materials and Methods.

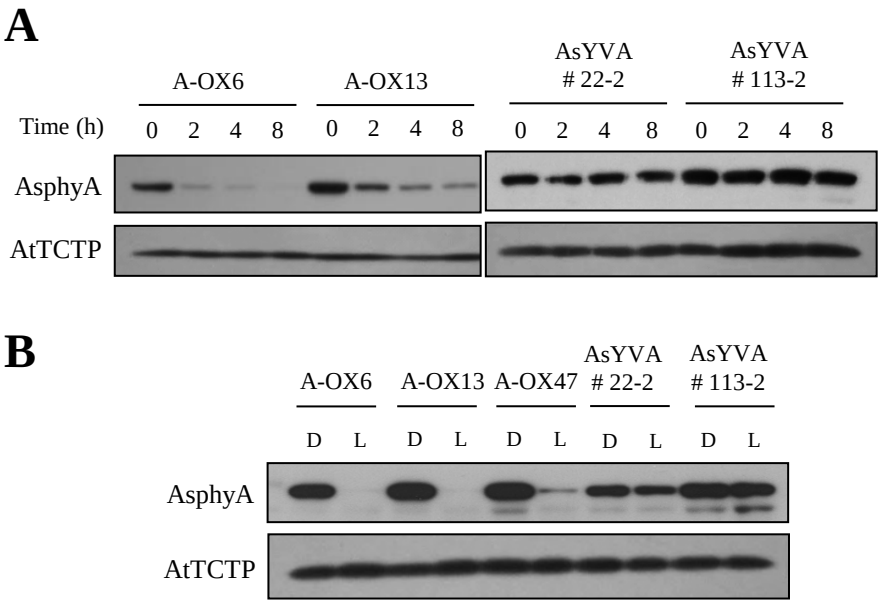

Supplemental Figure S9. Protein stability of AsYVA in plants. (A) Time-dependent degradation of AsphyA proteins under R light. 3.5 d-old dark-grown seedlings were irradiated with continuous R light (28 µmol m^{-2} s^{-1}) for the indicated periods of time. AtTCTP was shown as loading controls. **(B)** Comparison of AsphyA degradation under dark and light conditions. 3.5 d-old dark-grown seedlings of transgenic plants were grown in the dark (D) or irradiated with continuous white light (L; 150 µmol m^{-2} s^{-1}) for 24 h.

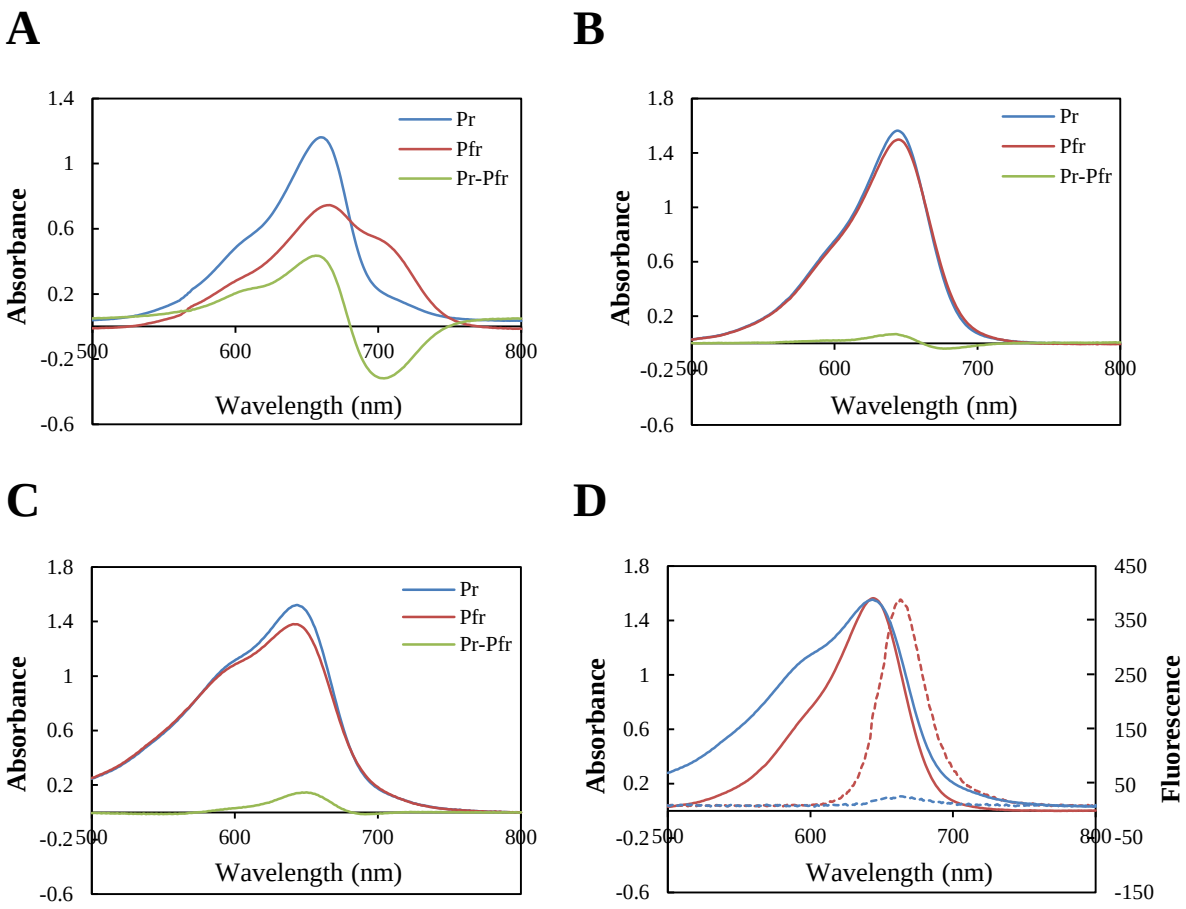

Supplemental Figure S10. Photochemical analyses of purified recombinant Cph1 mutant proteins. **A-C**, Absorbance and difference spectra of wild-type (A), Y176H (B), and Y203V (C) of Cph1. Pr (blue)/Pfr (red) absorbance spectra and difference spectra (green) were shown. Both mutants were poorly photoactive, exhibiting significantly reduced difference spectra, compared with wild-type Cph1. **D**, Absorption spectra (solid lines) and fluorescence emission spectra (dotted lines) for Y176H (red) and Y203V (blue). The Y176H mutant exhibited enhanced fluorescence with an emission maximum at 664 nm in our experimental conditions. In contrast, we could not observe the enhanced fluorescence with the Y203V mutant, as well as with the Y203H mutant (data not included, because the fluorescence emission spectra of Y203V and Y203H were similar).

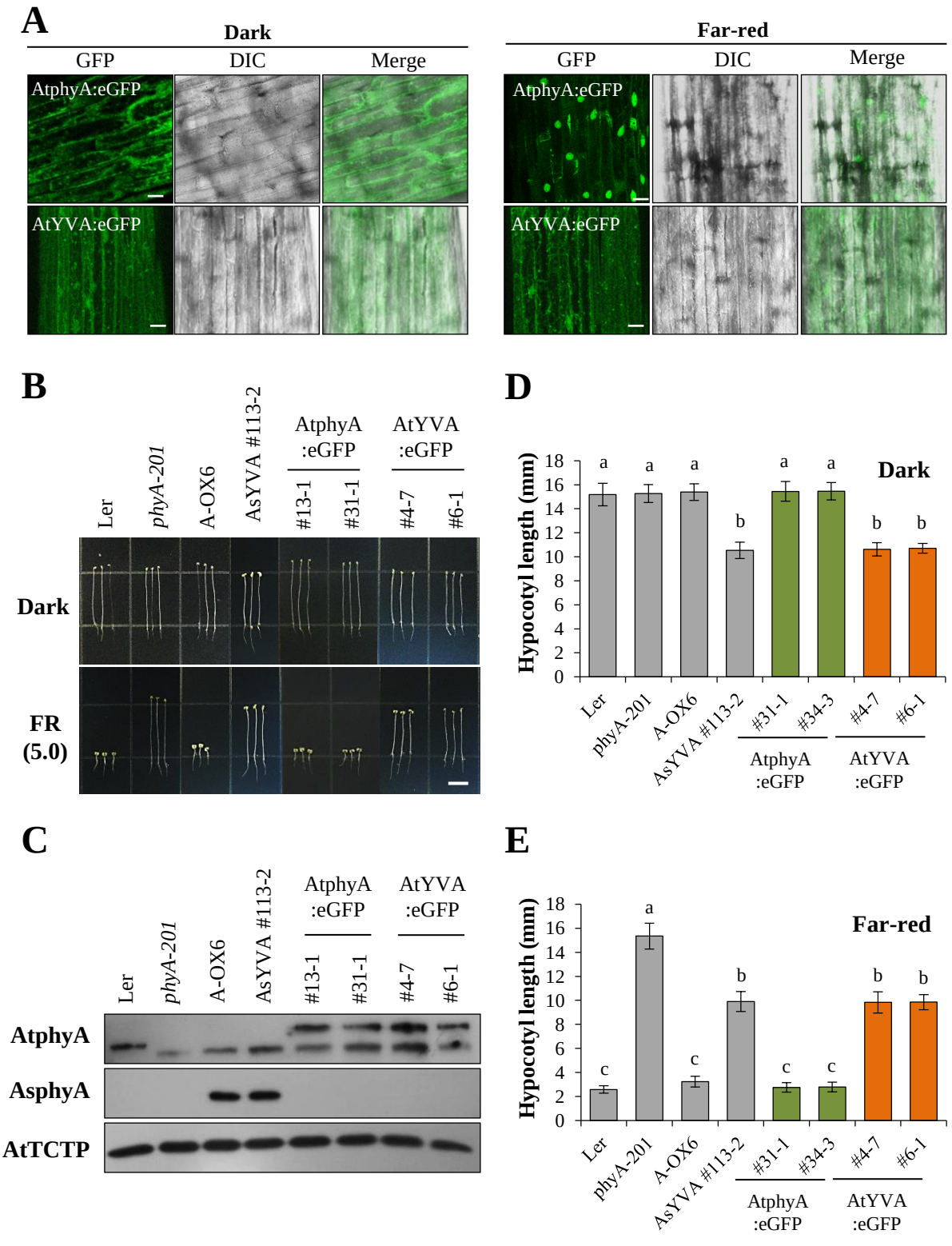
A
Dark
GFP
DIC
Merge
AtphyA:eGFP
AtYVA:eGFP
Far-red
GFP
DIC
Merge
AtphyA:eGFP
AtYVA:eGFP
B
Ler
phyA-201
A-OX6
AsYVA #113-2
AtphyA :eGFP
AtYVA :eGFP
#13-1
#31-1
#4-7
#6-1
Dark
FR (5.0)
D
Dark
Hypocotyl length (mm)
Ler
phyA-201
A-OX6
AsYVA #113-2
#31-1
#34-3
#4-7
#6-1
AtphyA :eGFP
AtYVA :eGFP
C
Ler
phyA-201
A-OX6
AsYVA #113-2
AtphyA :eGFP
AtYVA :eGFP
#13-1
#31-1
#4-7
#6-1
AtphyA
AsphyA
AtTCTP
E
Far-red
Hypocotyl length (mm)
Ler
phyA-201
A-OX6
AsYVA #113-2
#31-1
#34-3
#4-7
#6-1
AtphyA :eGFP
AtYVA :eGFP

Supplemental Figure S11. Subcellular localization and photoresponse analyses of AtYVA. **A**, Subcellular localization analysis. Three-day-old dark-grown transgenic seedlings were kept in the dark or exposed to far-red light (5.0 μmol m^{-2} s^{-1}) for 1 h. AtphyA:eGFP, transgenic *phyA-201* lines with eGFP-fused wild-type AtphyA; AtYVA:eGFP, transgenic *phyA-201* lines with eGFP-fused Y269V-AtphyA. Scale bar = 10 μm. **B**, Seedling de-etiolation responses of transgenic plants under dark or continuous far-red light (5 mol m^{-2} s^{-1}). Scale bar = 5.0 mm. **C**, Immunoblot analysis to show AtphyA protein levels in transgenic plants. AtphyA-specific (agrisera), AsphyA-specific (oat25), or AtTCTP-specific antibody was used for the immunoblots. The lower bands in the upper panel represent truncated AtphyA proteins in *phyA-201* that was used for transformation. **D-E**, Average hypocotyl lengths of seedlings in (B). Data are the means ± SD ($n \geq 25$). Means with different letters are significantly different at $P < 0.01$, using Duncan's multiple range test.

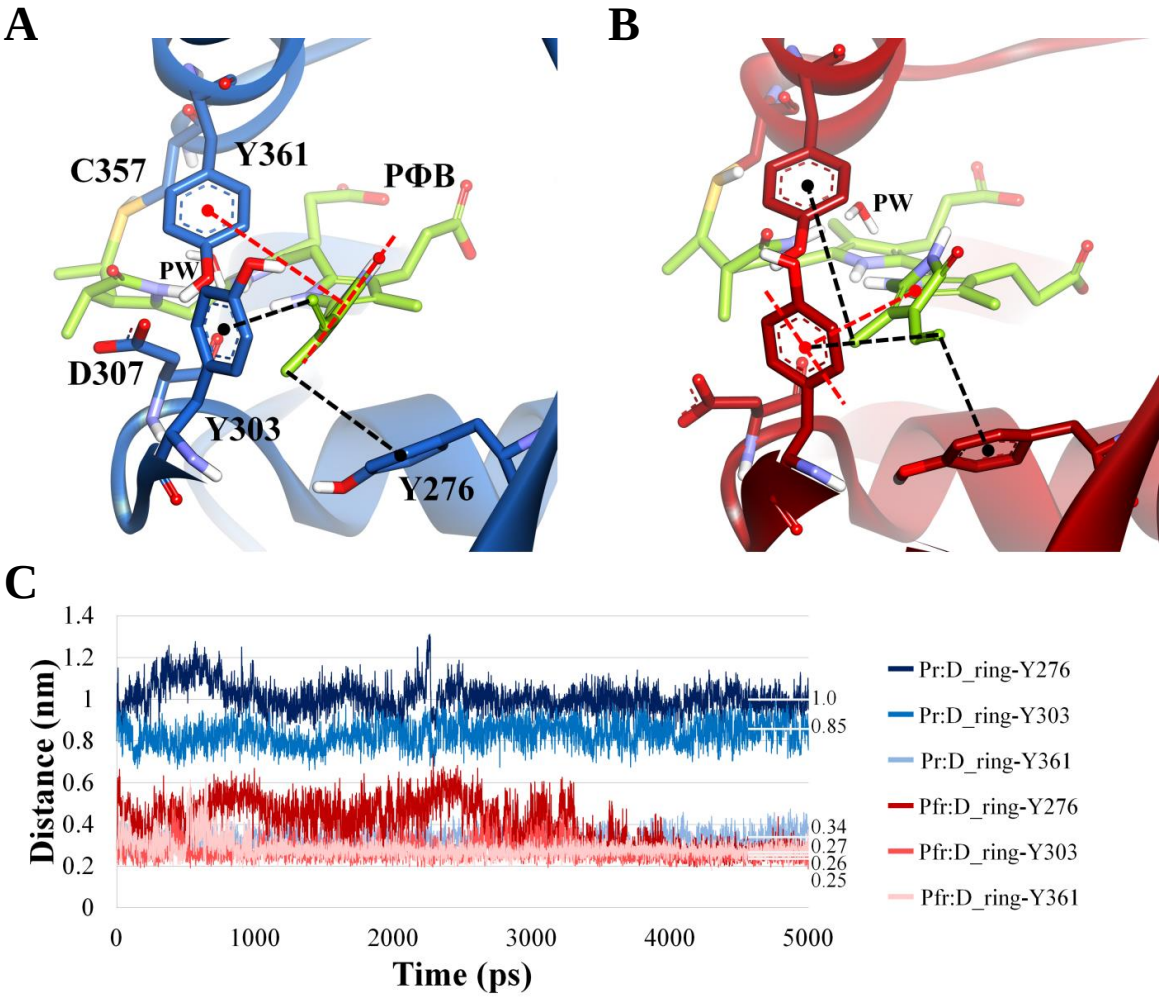

Supplemental Figure S12. Prediction for the positions of tyrosine residues near the D-ring of chromophore in the Pr and Pfr forms of AtphyB. **A-B**, The predicted chromophore binding modes in the Pr (blue) and Pfr (red) forms of AtphyB. The secondary structures of proteins are depicted as ribbon models, and the phytochromobilin (PΦB) molecule was included as a chromophore (green). The PΦB-interacting residues and the pyrrole water (PW) were labeled and represented as stick models. For amino acid residues, oxygen, nitrogen, hydrogen, and sulfur atoms are in red, blue, white, and yellow, respectively. The T-shaped π-π interaction and alkyl-π interactions are shown as red-dashed and black-dashed lines, respectively. **C**, Distance measurement between three tyrosine residues and D-ring of PΦB in the Pr and Pfr forms of AtphyB. For each tyrosine residue, the distance to the center of D-ring was averaged during the last 1 ns of the MD simulations.